

and I profiles (for the crown block located at the upper part of the mast). The entire high of the laboratory model of the mast is about 3 meters. An overall view of this model is presented in figure 1 and the calculation model in figure 2.



Fig. 1 The laboratory model

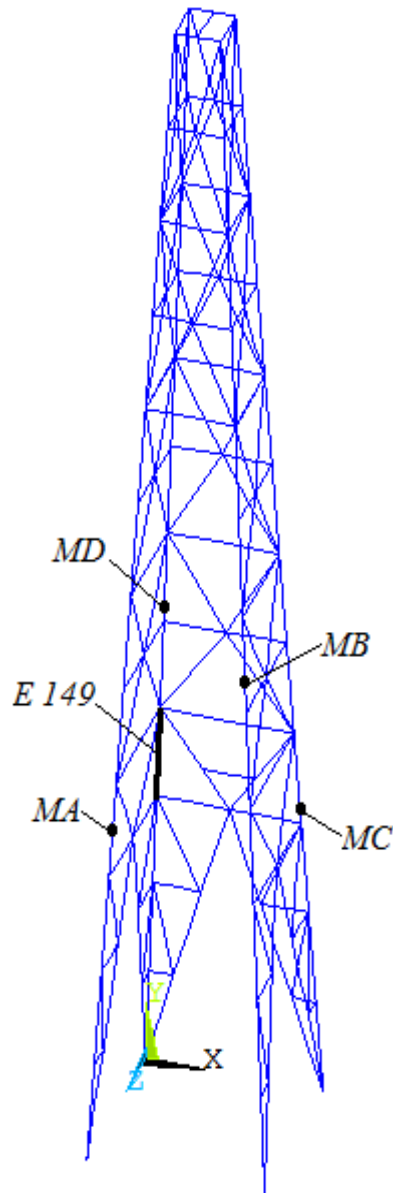


Fig. 2 The FEA calculation model

The static and dynamic analysis have been carried out using the FEA ANSYS software. The laboratory tests have been completed using a modern acquisition system that collects the signal from strain gauges and provides the strains in the points where the strain gauges are connected with the steel (see fig.2, element 149) In figure 2 can be noticed the pillars of the mast (MA, MB, MC and MD – presented above).

The main structure of the mast is composed from four identically pillars, made of $\phi 8 \times 0.3$ pipes, manufactured from S235 JR steel (SREN10025-2004), two of them located in the front side of the mast and the others in the back. The lower part of the mast is designated to support the entire structure and is usually the most stressed area. The upper part of the mast contains also some horizontal and diagonal bars covering in their assembly four stages (Fig.2) in which the diagonals are griped in a X shape.

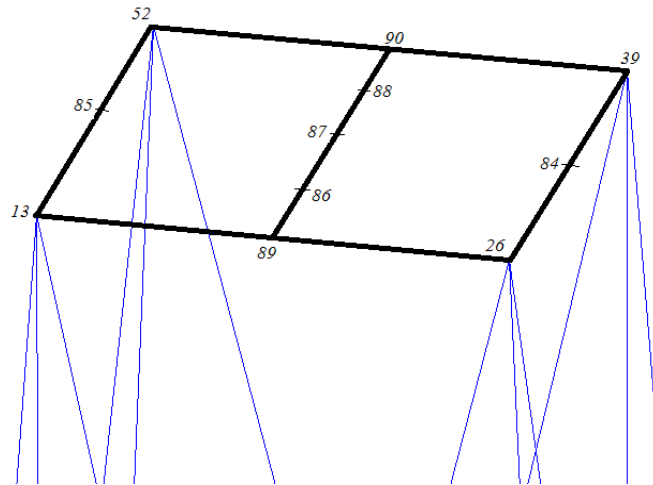


Fig. 3 The crown block of the mast

The crown block (Fig.3) located at the top of the mast contains many strong horizontal bars made from I profile (22 x 17 x 3). All the bars from the mast are rigidly held at their ends, by welding.

2. THE FEA MODEL

Because the mast represents a multiple statically undetermined structure, the finite element analysis has been followed, by making use of ANSYS software, using the same methodology presented in (Stanciu-2014, Popa-2014). Each beam of the entire structure has been meshed into finite elements (BEAM 189) resulting a total number of 232 isoperimetric elements and 185 connecting nodes. In order to complete a general study of the strength behavior of the mast a statically and post dynamically analysis have been carried out. The main aims of the above analysis are divided in the following load cases:

- 1- to check the strength behavior of the mast loaded with a normal operating force (443 N) that can be measured in laboratory by using a digital force transducer; the stress appeared in element 149 (Fig.2) was also experimentally verified by using a modern strain gauges acquisitions system;
- 2- to find the maximum force that produces in mast the highest allowable limit of the material;
- 3- to find the dynamic response of the mast to a dynamic force produced during the overload test, when the external weight of the load mass is lowered down to the hook.

According with the main regulations from actual standards in range for metallic structures (*EN 10025-2-2004*) the main values of forces acting on the entire structure (for load cases 1 and 2) are presented in table 1 below, where are also specified the number of the corresponding nodes from Fig.3 (where the external forces act).

Table 1. Values of the external forces acting the mast

Load case	External force [N]	Node no.	Force direction	Nodal force value [N]
1	443	84	FY	-110.75
		84	FZ	-12
		85	FY	-110.75
		85	FZ	-15
		86	FY	-110.75
		87	FY	-110.75
		88	FY	-110.75
2	3520	84	FY	-880
		84	FZ	-96
		85	FY	-880
		85	FZ	-120
		86	FY	-880
		87	FY	-880
		88	FY	-880

As it can be noticed from the values presented in table 1 there are some small horizontal components that appear due to the draw works, drum socket and the blind end of the rotary line. Also the vertical values of the operating and maximum forces have multiplied with a 1.2 coefficient because of the supplementary weight produces by the hoisting system (hoisting crane, hook and cables),

3. THE FEA STATIC RESULTS

Because the mast represents a multiple statically undetermined structure, the finite element analysis has been followed, by making use of ANSYS software (*ANSYS User Guide*). Each beam of the entire structure has been meshed into finite elements (BEAM 189). As a result of the static calculation **for the first load case** it can be noticed that the maximum tension stress appears in the horizontal bar that connects the MA and MC pillars (marked with Z3 in Fig.4) and has the value $\sigma_{max} = 11.54 \text{ MPa}$. The maximum compression stress appears at the bottom of the MD pillar, in the supporting area (marked with Z4 in Fig.4) and has the value $\sigma_{min} = -18.54 \text{ MPa}$. On the element E149 where a strain gauge has been located, the axial stress is $\sigma_{x,149} = -13.98 \text{ MPa}$.

The maximum displacement along horizontal z axis is reached at the top of the mast, at the crown-block level and has the value: $u_z = -0.32 \text{ mm}$. The most significant

displacements are along z direction and the deformed shape of the mast is presented in Fig. 5

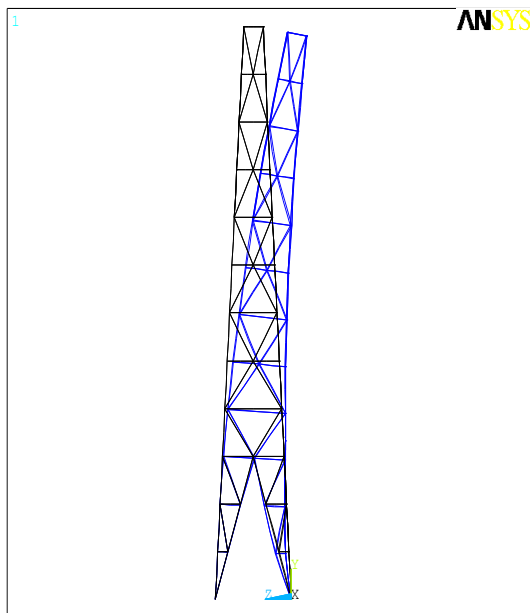
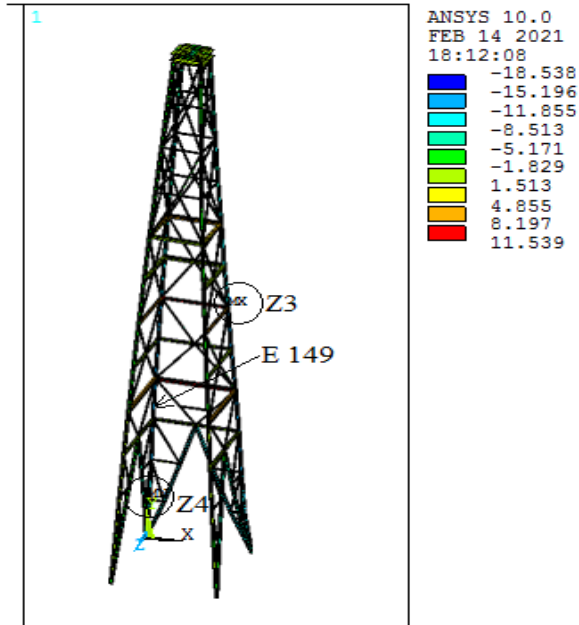


Fig.4 The most stressed areas
mast

Fig. 5. The deformed shape of the

In order to verify the numerical results presented above an experimentally work has been completed. This is also required because in the last period of time the main international regulations (especially *API 4F, 2013 Edition*) accept that the homologations of the structures can be carried on by using the FEA results instead of experimentally work.

In order to simulate the external load of the mast a DC motor with 24 V supply voltage and 5A current intensity has been used. The main purpose of the motor was to load the operating drum and through the crane-cable system to create the operating force to the hook. The force has been registered (during the loading process) with a digital force transducer presented in Fig. 6. The screen of the transducer is presented in Fig. 7,

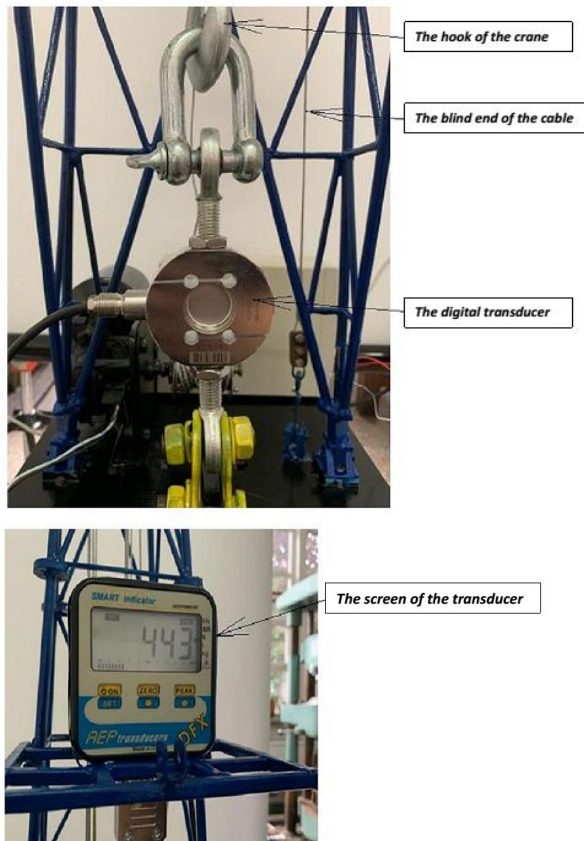


Fig. 6. The force transducer

Fig.7. The screen of the transducer

During the loading process (realized with the DC motor) the signals from the strain gauge located on element $E149$ (Fig. 2) have been permanently registered and processed with a modern acquisition system softened with the STRAIN SMART 8000 program. The variation of the strains against time is presented in Fig. 8 below where is specified also the point that corresponds to the operating force (443 N).

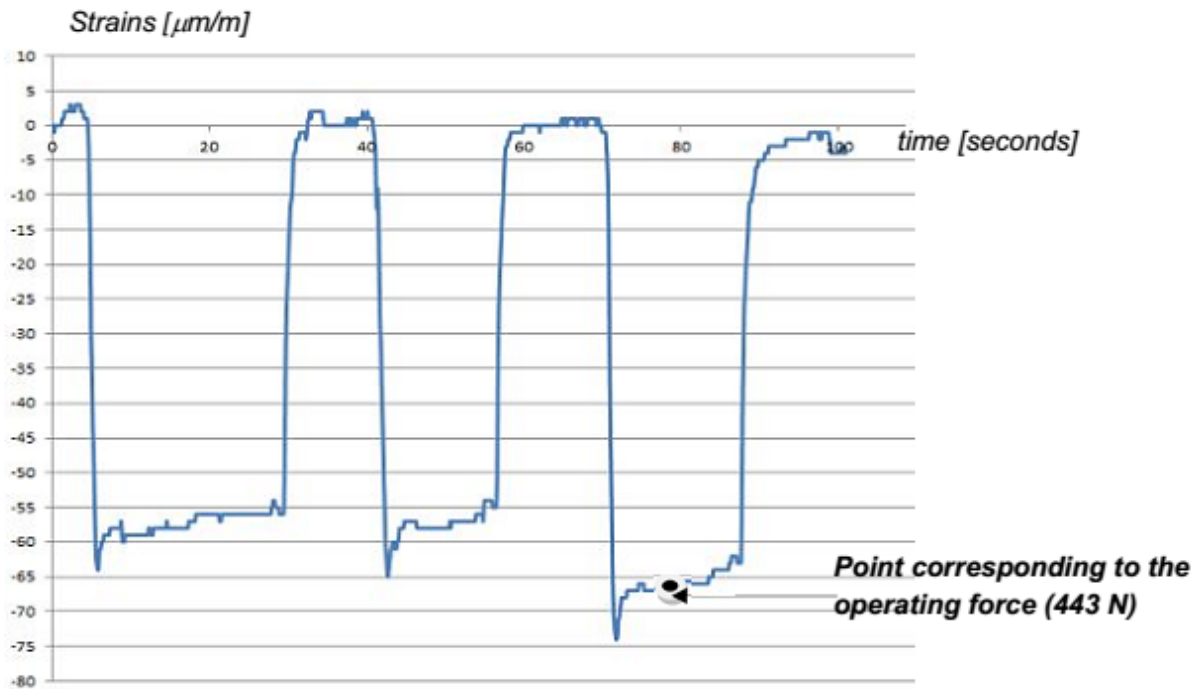


Fig. 8. The strain variation against time

From the variation presented above (in Fig. 8) it can be noticed that, when the mast is loaded with the operating force (443 N) the strain provided by the strain gauge (in element *E149*) is $\varepsilon_x = -67 \mu\text{m/m}$. Using the axial Hooke's law the corresponding experimental axial stress in element *E149* is:

$$\sigma_{x,\text{exp}} = E \cdot \varepsilon_x^* = 2.1 \cdot 10^5 \cdot 67 \cdot 10^{-6} = -14.07 \text{MPa} \quad (1)$$

Comparing the experimental and numerical values from the axial stresses from the element *E149* ($\sigma_{x,\text{exp}} = -14,07 \text{MPa}$ and $\sigma_{x,149} = -13,98 \text{MPa}$) it can be noticed a very good approach of the above values, the relative error between them being 0.6%. This very good approach between experimental and numerical values could be a good reason to use proper FEA models instead of experimental work (recommendation of *API 4F, 2013 Edition*).

The second load case uses the same calculation model and the external forces (see table 1) have been increased until the allowable limit of the material has been reached in the structure. This phenomenon happens when the vertical force from the hook reaches the value of 3520 N.

As a result of the static analysis the distribution of the stresses are presented in Fig. 9.

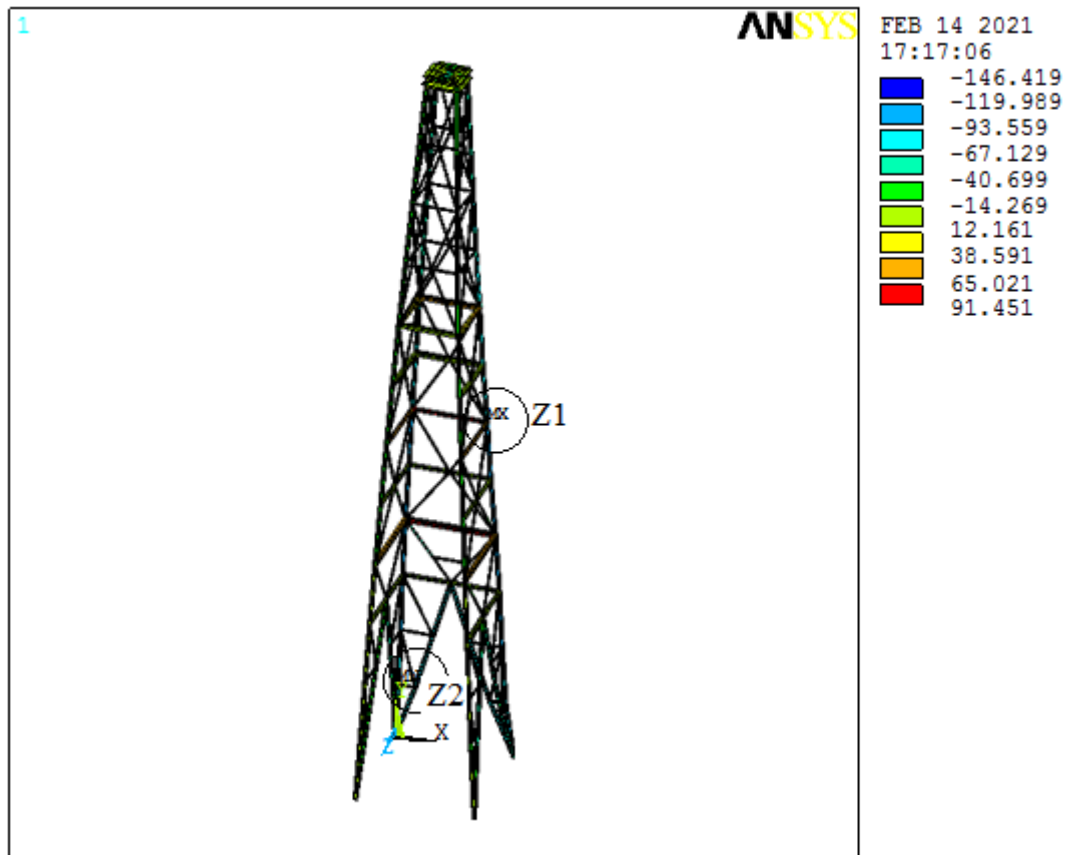


Fig. 9. The stress distribution in load case 2

From the map presented above it can be highlighted two areas : Z1 corresponding to the maximum tensions and Z2 to the maximum compressions. The maximum tensions reached in Z1 area appear in a horizontal beam that connects the MC and MD pillars and has the value of 91.45 MPa (Fig.9). The maximum compressions reached in Z2 area appear in an element located at the bottom of the structure and has the value -146.42 MPa . The maximum displacement along horizontal z axis appears at the top of the mast and has the value: $u_z = -2.61 \text{ mm}$. The deformed shape of the entire structure is the same with those presented in Fig. 5.

4. THE FEA POST DYNAMIC RESULTS

From the above static analysis (especially from load case 2) has been concluded that the maximum extra load (test load) of the entire structure cannot be higher than 3520 N. This value has to be connected with the maximum allowable test values that are recommended in (API 4F) but cannot exceed the above value provided by load case 2. For this reason **the load case 3** analyzes the dynamic effect that appears when the extra load weight is lowered to the hook.

The post dynamic analysis provides the dynamic response (in displacements) for the maximum force calculated in load case 2 (3520 N). The first ten natural angular

frequencies are presented in table 2 below. The third row of the table presents the most important oscillation that characterizes the respective proper mode.

Table 2- The first ten natural angular frequencies of the mast

f1 [rad/s]	f2 [rad/s]	f3 [rad/s]	f4 [rad/s]	f5 [rad/s]	f6 [rad/s]	f7 [rad/s]	f8 [rad/s]	f9 [rad/s]	f10 [rad/s]
268.5	288.1	529.9	534.5	685.8	876.3	990.6	1206.7	1219.7	1344.4
Oscillation in xOy plane	Oscillation in xOz plane	Torsional oscillation	Oscillation in xOy plane	Oscillation in xOy plane	Oscillation in xOy plane	Oscillation in xOy plane	Oscillation in xOz plane	Oscillation in xOy plane	Oscillation in xOy plane

In order to obtain the dynamic response of the entire structure to the effect of lowering the weight into the hook it is necessarily to consider at least eight proper modes of vibration because the most important displacements of the mast are in z direction (in xOz plane). The study is carried out considering a 0.029 damping coefficient for the first mode of vibration. For the others the damping coefficients are calculated using the method presented in (Posea -1994). The dynamic u_z response for the corner point located at the top of the mast (point no 39 - Fig. 3) is presented in figure 10 below.

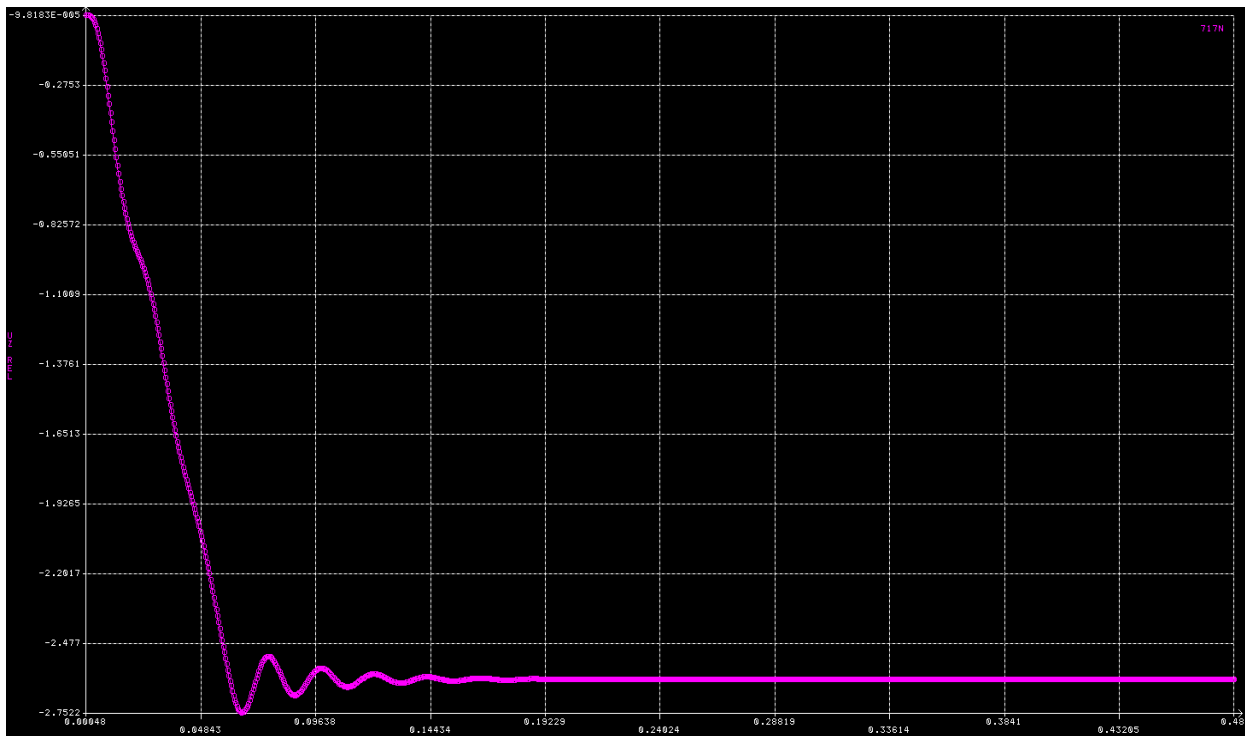


Fig. 10 The dynamic response in u_z displacements

From the data presented in Fig. 10 it can be noticed that the maximum u_z displacement appeared as a dynamic effect of lowering the test weight into the hook is 1.054 higher

than the static displacement of the same points (2.75 mm against 2.61 mm). The above value can represent a reduction coefficient (c_r) that is recommended to be applied to the maximum value of vertical force in order to reach the overload test situation of the structure.

This means that the maximum test load of the mast cannot exceed the value:

$$F_{mac} = \frac{F}{c_r} = \frac{3520}{1.054} = 3340N$$

(2)

If the weight of the test is lowered to the hook from a height (h) the reduction coefficient (c_r) has to be multiplied with the usual shock dynamic coefficient (Posea -1994) and the maximum value of the test load will become lower.

From the Fig. 10 it can be also noticed that the dynamic response becomes stabilized after 0.2 seconds time after that the mast recovers its static behavior. It must also be mentioned that the reduction coefficient for our laboratory mast has a small value because of small values of horizontal forces and height of the mast. It is appreciated that for industrial structures, especially for transportable masts, the value of the reduction coefficient will be more significant. For this reason a post dynamic analysis is recommended for every industrial structure, following the methodology presented above.

5. CONCLUSIONS

The development of the onshore structures required in the last period of time more detailed analyses of the drilling equipment. Interesting technical studies that use the Finite Element Analysis (FEA) are provided in the last ten years by Chinese researchers-see for example Guo (2011) and Li (2012).

In the paper are presented a static and a dynamic analysis of a laboratory mast manufactured after an industrial model. The entire study has been carried out using the FEA (ANSYS) and can be divided into three load cases:

- **load case 1** presents the static behavior of the structure subjected with a normal operating force provided by a DC motor. The axial stresses appeared in a beam located at the bottom of the structure are also experimentally verified. The very good concordance between numerical and experimental results justifies the actual regulations (API 4F, 2013 Edition) that accepts for masts the using of FEM instead of experimental work;
- **load case 2** finds the maximum force that produces in mast the maximum allowable limit of the material; for this case the maximum displacements for some points located at the top of the structure are highlighted;
- **load case 3** deals with a modal and post dynamic analysis that provides the first ten natural frequencies of the mast and the dynamic responses (in displacements) for some points located at the top of the structure. The dynamic behavior of the mast is produced by the effect of lowering the test weight into the hook and for this load case a reduction coefficient (of the testing force) is defined.

The maximum value of the test load of the mast cannot exceed the maximum static value of the force (expressed in load case 2) divided by the reduction coefficient calculated in the load case 3. If the test load is lowered into the hook from a specified height the reduction coefficient has to be multiplied with the usual value of the shock coefficient.

The third stage of this study is recommended to complete the regulation from API 4F (2013 Edition) in order to establish precisely (for every industrial structure) the dynamic reduction coefficient produced by lowering the test weight into the hook.

REFERENCES

- Lambrescu, I. and Pana, I. (2014), "Theoretical and experimental fatigue analysis for the mast MU450 top drive drilling mast with impact on the reliability", *Proceedings of the Balkantrib, the 8th International Conference on Tribology, Sinaia, Romania*, 656-664.
- Pana, P. and Babe, P. (2011), "Drilling Rigs Modelling Using AVEVA PDMS Software", *J. of Petroleum-Gas University of Ploiești, Technical series*, LXIII(3), 5-13.
- Popa, I and Stanciu, L. (2014), "Stress and displacements analysis for drilling mast elements made of rectangular pipe: the overload test case", *Key Engineering Materials*, 601, 120-123.
- Posea, N., Anghel, A. and Popa I. (1994), "The Dynamic Calculation of Structures" (in Romanian), *Dydactical and Pedagogical Pub. House, Bucuresti, Romania*.
- Stanciu, L. and Popa, I. (2014), "Stress and Displacements Analysis for Drilling Mast Elements Made of Rectangular Pipe under the Action of the Wind as a Hurricane", *Key Engineering Materials*, 601, 116-119.
- Vasilescu, S. (2012), "An Approximate Method Used in the Calculation of the Critical Load for Beams with Variable Cross Sectional Area" (in Romanian), *J. of Petroleum-Gas University, Technical Series*, LXIII(3), 23-29.
- Guo, H. and Zang, H.L. (2011), "Finite element method analysis of the mast of rotary drilling rig", *Advanced Materials Research*, 374-377, 326-329.
- Li, Y.X., Xia, W.Q., Shen, W.Q. and Luo, H. (2012), "Structural Optimum Design and Analysis of the Mast of Rotary Drilling Rig Based on Finite Element Method", *Research Journal of Applied Sciences, Engineering and Technology*, 4, 3222-3230.
- API 4F, 2013 Edition, "Specifications for Drilling and Well Servicing Structures", *API energy, Washington*.
- ANSYS Release 10.0 Software.
- EN 1991-1-4, 2007 Edition, "Action on structures", Part 1-4: General actions- Wind actions.
- STAS 1909 (1989), "Derricks and masts for drilling and intervention" (in Romanian).
- EN 1993-1, Eurocod 3: Design of steel structures (in Romanian).
- EN 10025-2 (2004), Hot Rolled Products of Structural Steel.
- SR 438-1(2012), Steel Products for Concrete Reinforcement (in Romanian).